Journal Pre-proof

Influence of substituting Na^{+} for Mg^{2+} on the crystal structure and microwave dielectric properties of $Mg_{1-x}Na_{2x}WO_4$ ceramics

Qin Zhang, Xiaoli Tang, Yuanxun Li, Yulan jing, Hua Su

PII: S0955-2219(20)30404-0

DOI: https://doi.org/10.1016/j.jeurceramsoc.2020.05.053

Reference: JECS 13298

To appear in: *Journal of the European Ceramic Society*

Received Date: 16 December 2019

Revised Date: 19 May 2020

Accepted Date: 20 May 2020

Please cite this article as: { doi: https://doi.org/

Influence of substituting Na^+ for Mg^{2+} on the crystal structure and microwave dielectric properties of $Mg_{1-x}Na_{2x}WO_4$ ceramics

Qin Zhang[1], Xiaoli Tang[1], Yuanxun Li[1,2], Yulan jing[1], Hua Su[1,2*]

[1]*State Key Laboratory of Electronic Thin Films and Integrated Devices, University of Electronic Science and Technology of China, Chengdu, 610054, China*

[2]*Jiangxi Guo Chuang Industrial Park Development Co., Ltd, Ganzhou, China.*

**Corresponding author: uestcsh77@163.com*

Highlights

- Na^+ substitution effectively lowered sintering temperature and contributed to the optimization of Q × f value.
- The dielectric constant tended to decrease, which was more conducive to signal transmission.
- The τ_f value was closely related to the distortion of [MgO_6] octahedron.
- Excellent dielectric properties were exhibited at x=0.06 with ε_r= 10.474, Q×f = 45,868 GHz, and τ_f = −69 ppm /ºC.

Abstract

The $Mg_{1-x}Na_{2x}WO_4$ ($0 \leq x \leq 0.14$) microwave dielectric ceramics were prepared through traditional solid-state reaction and sintered at 875-925 °C for 4 h. Compared with pure $MgWO_4$ ceramic, the samples with substituting Na^+ for Mg^{2+} could be sintered at a lower temperature, the quality factor values and the densification of microstructure were obviously improved. Raman spectroscopy proved that the relative permittivity was related to the multiple phases and molecular polarizability. In addition, the distortion of

$[MgO_6]$ octahedron also changed, resulting in resonance frequency temperature coefficient varied nonlinearly from $x = 0$ to 0.14. Considering the applications of low temperature co-fired ceramics technology, the $Mg_{1-x}Na_{2x}WO_4$ ($x = 0.06$) ceramic sintered at 875 °C had the best performance. Not only did it have excellent microwave dielectric properties of $\varepsilon_r = 10.474$, $Q \times f = 45{,}868$ GHz, and $\tau_f = -69$ ppm /ºC, but also presented great chemical compatibility with the commonly used Ag electrode.

Keywords: *$Mg_{1-x}Na_{2x}WO_4$ ceramics; Na^+ substitution; microwave dielectric properties; LTCC*

1. Introduction

With the rapid development of microwave communication technology, the miniaturization, integration, and multifunction of electronic devices are increasingly required. Low temperature co-fired ceramics (LTCC) technology has become the most concerned direction of microwave integration discovery because of its characteristics

of high integration, multi-function and low cost [1]. As a substrate material, LTCC has low dielectric constant, high quality factor and near-zero resonant frequency temperature coefficient, and widespread uses in automotive electronics, communications, aerospace, military and other fields [2-4]. In addition, the sintering temperature of LTCC should be lower than the melting point of Ag (961°C), which is often used as the electrode in LTCC technology [5, 6]. Therefore, the development of microwave dielectric ceramics with excellent properties and low sintering temperature has become an important topic.

The tungstate microwave dielectric ceramics have been widely studied because of their low sintering temperature and low dielectric constant, such as $CaWO_4$ ceramic ($Q\times f$ =70,000GHz, ε_r=10.4), $BaWO_4$ ceramic ($Q\times f$ =57,500 GHz, ε_r =8.1) and $SrWO_4$ ceramic ($Q\times f$ =62,600 GHz, ε_r =9.0) [7]. $MgWO_4$ ceramic is also a potential excellent LTCC material with low dielectric constant (ε_r=12-14) and high $Q\times f$ value. When sintered at 1050 °C, $MgWO_4$ ceramic presented excellent dielectric properties: ε_r=13.5, $Q\times f$ = 69,000 GHz, andτ_f= -58 ppm /°C [7]. However, the sintering temperature of $MgWO_4$ was too high to be co-fired with silver electrode, which limited the application of $MgWO_4$ in LTCC technology. In addition, Pullar et al. found that $Q\times f$ value of $MgWO_4$ was only 5400 GHz when sintered at 950 °C, indicating that the low-temperature sintering performance of $MgWO_4$ was very poor [8]. Therefore, to obtain the excellent dielectric properties of $MgWO_4$ and lower its sintering temperature, appropriate methods should be adopted. In general, the sintering temperature of LTCC materials can be reduced by three methods: using ultrafine particles as raw materials through advanced chemical processes, adding oxides with low melting points to replace ions, or adding glass fluxes.

Wang et al. confirmed that Na^+ substitution had a good effect on reducing the sintering temperature of $CaWO_4$ ceramics [9]. In this paper, Na^+ was used to substitute for Mg^{2+} to reduce the sintering temperature of the $Mg_{1-x}Na_{2x}WO_4$ ($0 \leq x \leq 0.14$) ceramics. A conventional solid-state reaction was used to produce the samples, and the phase composition, microstructure, and microwave dielectric properties of the samples were systematically studied.

2. Experimental procedure

The $Mg_{1-x}Na_{2x}WO_4$ (x = 0, 0.02, 0.04, 0.06, 0.08, 0.10, 0.12, 0.14) ceramics were prepared by the traditional solid-state reaction in which purity Na_2CO_3 (99.8%), nanometer MgO (99.8%), and WO_3 (99%) were used as raw materials. The mixed powders according to the compositions were weighted and placed into nylon tanks to wet milled for 4 h in distilled water by using zirconia balls as medium. The milled powders were dried and calcined at 800 °C for 2 h. Then the calcined powders were re-milled in nylon tanks for 6 h. After that, the powders were dried, mixed with 10% PVA (Polyvinyl alcohol), and granulated, which were final pressed into cylindrical samples and sintered at 875 °C -925 °C for 4 h.

Crystalline phases of the samples were confirmed by the X-ray diffraction analysis（XRD:DX-2700）using Cu Kα radiation at room temperature. The detailed structure refinements were obtained by using Fullprof program. The microstructure images of the polished and thermally etched surfaces were observed by a scanning electron microscope (SEM) (JSM-6490; JEOL, Japan). The Raman spectra were obtained using an InVia Raman microscope (Renishaw, UK) with an argon ion laser (λ = 514.5 nm) as the excitation light. Raman shifts were measured with a precision of ~0.3 cm^{-1}. The microwave dielectric properties of the samples were tested by Hakki–Coleman resonator method and Agilent N5230A network analyser (300MHz-20GHz)

in a resonant cavity, and the bulk volume densities were measured by Archimedes principle[10]. The τ_f (ppm/°C) values were calculated according to the following equation [5, 11]:

$$\tau_f = \frac{f(85°C) - f(25°C)}{(85-25) \times f(25°C)} \times 10^6 (\text{ppm/°C}) \quad (1)$$

3. Results and discussion

3.1 XRD analysis

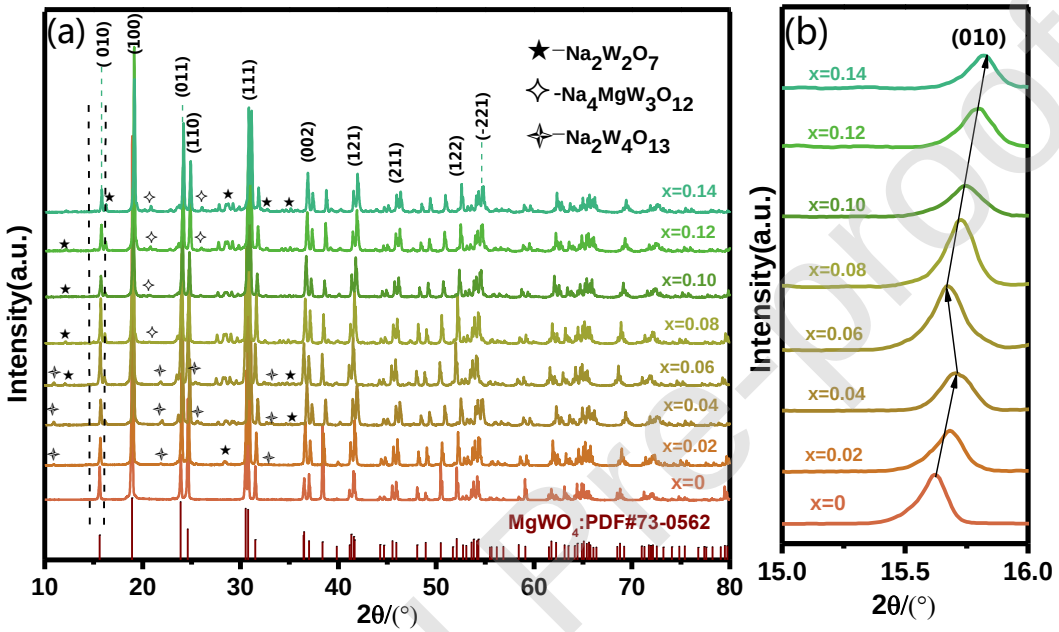

Fig. 1 (a) XRD patterns of the $Mg_{1-x}Na_{2x}WO_4$ ceramics sintered at 875 °C in various x value; (b) The amplified profile of the XRD patterns at around 15.75°.

The XRD patterns of the $Mg_{1-x}Na_{2x}WO_4$ ceramics sintered at 875 °C are presented in Fig. 1(a). The main phase and second phase were $MgWO_4$ (PDF#73-0562) and $Na_2W_2O_7$ (PDF#70-0860), the third phase was $Na_2W_4O_{13}$ (PDF#70-2022) when $x < 0.08$. According to Yuan et al.[12], the presence of $Na_2W_2O_7$ and $Na_2W_4O_{13}$ was partly due to the reaction of Na_2O-WO_3 binary system. Moreover, ionic substitution was related to ionic radius and electronegativity [13]. Due to the electronegativity difference between Na^+ and Mg^{2+} and different ionic radius (R_{Na^+} = 1.02 Å, $R_{Mg^{2+}}$ = 0.72 Å), no solid solution was formed. When $x \geq 0.08$,

the third phase changed from $Na_2W_4O_{13}$ to $Na_4MgW_3O_{12}$ (PDF#30-1216). This fact might due to that as the Na^+ substitution increased, the sintering temperature continued to decrease, which made the reaction between MgO and WO_3 easier.

3.2 Rietveld refinement

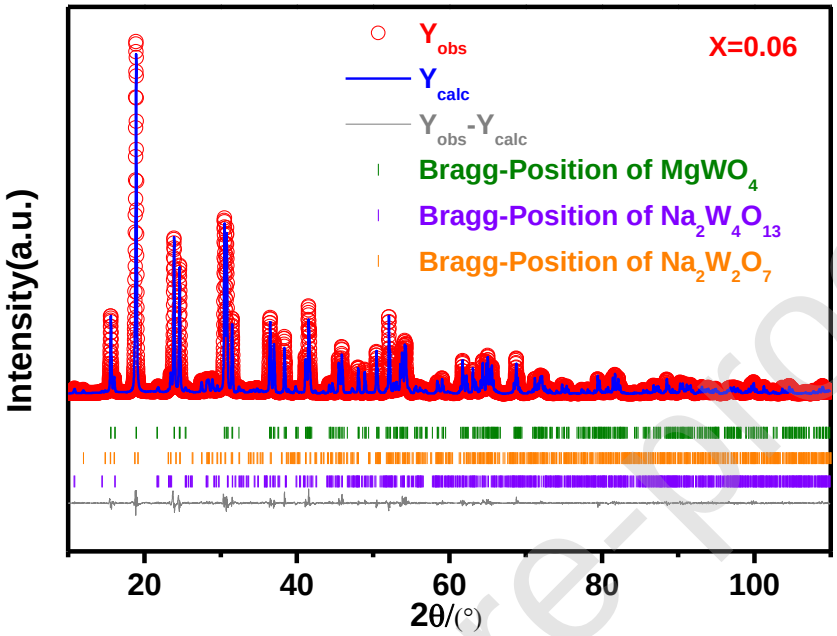

Fig.2 The Rietveld plot of the $Mg_{1-x}Na_{2x}WO_4$ (x=0.06) ceramics sintered at 875 °C.

To further investigate the influence of $Mg_{1-x}Na_{2x}WO_4$ ceramics' crystal structure on their microwave dielectric properties, the XRD data were refined using the Fullprof program [13]. Fig. 2 demonstrates the refinement patterns of the $Mg_{1-x}Na_{2x}WO_4$ (x=0.06) ceramic sintered at 875 °C. It was observed that the patterns calculated from the refined parameters closely agreed with the experimental data (see Supplementary Information Fig. S1 for more details), indicating that the refinement result was reliable. The refined crystal information of the $Mg_{1-x}Na_{2x}WO_4$ (x=0~0.14) ceramics is listed in Table S1. The lattice parameters of the samples were found to varied nonlinearly from x = 0 to 0.14, which also reflected by the shift of diffraction peak [14], as shown in Fig. 1 (b).

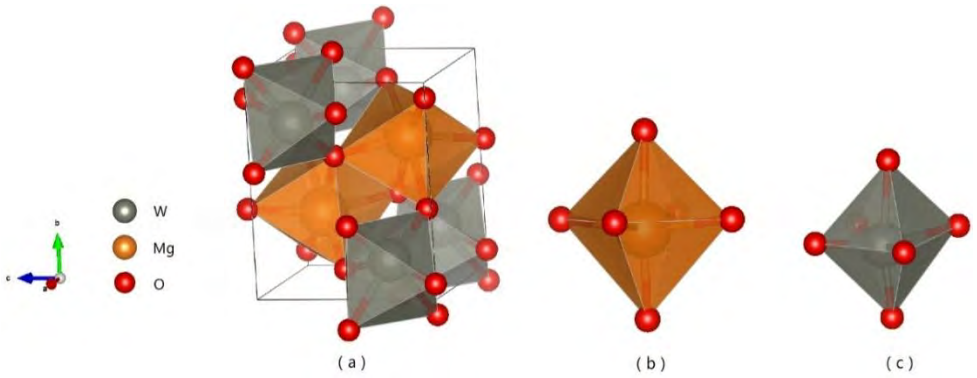

Fig.3 Schematic diagrams drawn with VESTA, (a) crystal structure of $MgWO_4$ ceramics in polyhedral style; (b) the structure of [MgO_6] octahedron; (c) the structure of [WO_6] octahedron.

The microwave dielectric properties of the $Mg_{1-x}Na_{2x}WO_4$ ceramics were influenced by crystal structure parameters of the main phase $MgWO_4$, such as octahedral deformation, bond ionicity, lattice energy and bond energy [15]. According to refinement results, the crystal structure of $MgWO_4$ obtained by Vestal software is shown in Fig. 3. The Mg^{2+} occupied the Wyckoff position (2f) and coordinated with six oxygen atoms to form an Mg-O octahedron; W^{6+} occupied the Wyckoff position (2e) and coordinated with six oxygen atoms to form a W-O octahedron; Two kinds of O^{2-} were present in this crystal cell, and both occupied the Wyckoff position (4g).

3.3 Density and scanning electron microscopy analysis

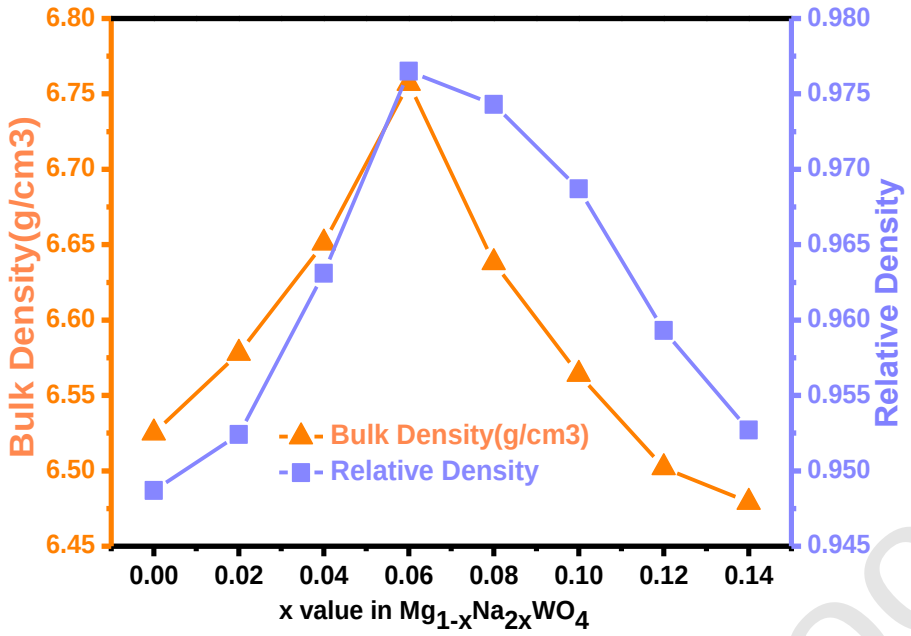

Fig.4 The relative density and bulk density of the $Mg_{1-x}Na_{2x}WO_4$ ceramics sintered at 875 °C in various x value.

As shown in Fig. 4, the variation in the relative density of the samples sintered at 875 °C was consistent with that of the bulk density. The bulk density of the $Mg_{1-x}Na_{2x}WO_4$ ceramics with a regular shape was calculated by Archimedes principle, and the theoretical density was determined via the following equation [16]:

$$\rho_1 = \frac{n \times A}{V \times N} \quad (2)$$

where n, A, V, and N were the number of formula units in a primitive cell, the molar masses of the composition, unit cell volume and Avogadro constant, respectively. In the three-phase system, the theoretical density was determined by the following equation [17]:

$$\rho_{theo} = (w_1 + w_2 + w_3)\left(\frac{W_1}{\rho_1} + \frac{W_2}{\rho_2} + \frac{W_3}{\rho_3}\right)^{-1} \quad (3)$$

where ρ_1, ρ_2, ρ_3, w_1, w_2, and w_3 represent the theoretical density and weight fraction of each phase. In addition, the relative densities of the compact ceramics were obtained from [18]:

$$\rho_{relative} = \frac{\rho_{bulk}}{\rho_{theo}} \quad (4)$$

The relative densities varied from 94.87%-97.65%, which indicated that the $Mg_{1-x}Na_{2x}WO_4$ ceramics were highly dense when sintered at 875 °C.

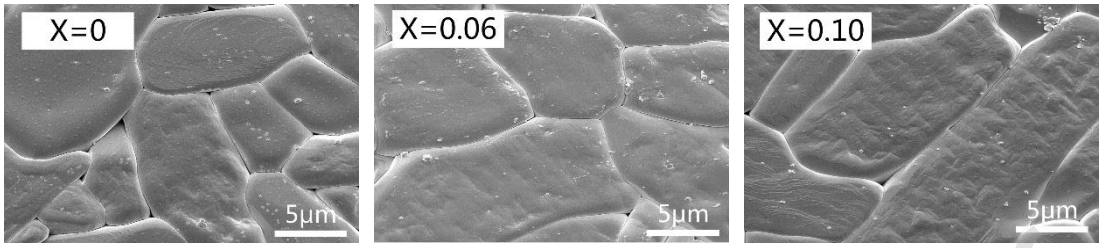

Fig.5 The SEM images on the polished and thermally etched surfaces of the $Mg_{1-x}Na_{2x}WO_4$ (x=0, 0.06, 0.10) ceramics sintered at 875 °C

Fig.5 shows the SEM images on the polished and thermally etched surfaces of the $Mg_{1-x}Na_{2x}WO_4$ (x=0, 0.06, 0.10) ceramics sintered at 875 °C. It could be seen that heterogeneity of grain size and evident pores were observed in the sample without Na^+ substitution. Compared with x=0, the grain size of the sample with x= 0.06 became larger and the microstructure became more uniform. However, abnormal grain growth occurred when Na^+ content further increased (x=0.10). It showed that moderate content of Na^+ substitution for Mg^{2+} facilitated a denser microstructure.

3.4 Raman spectra study

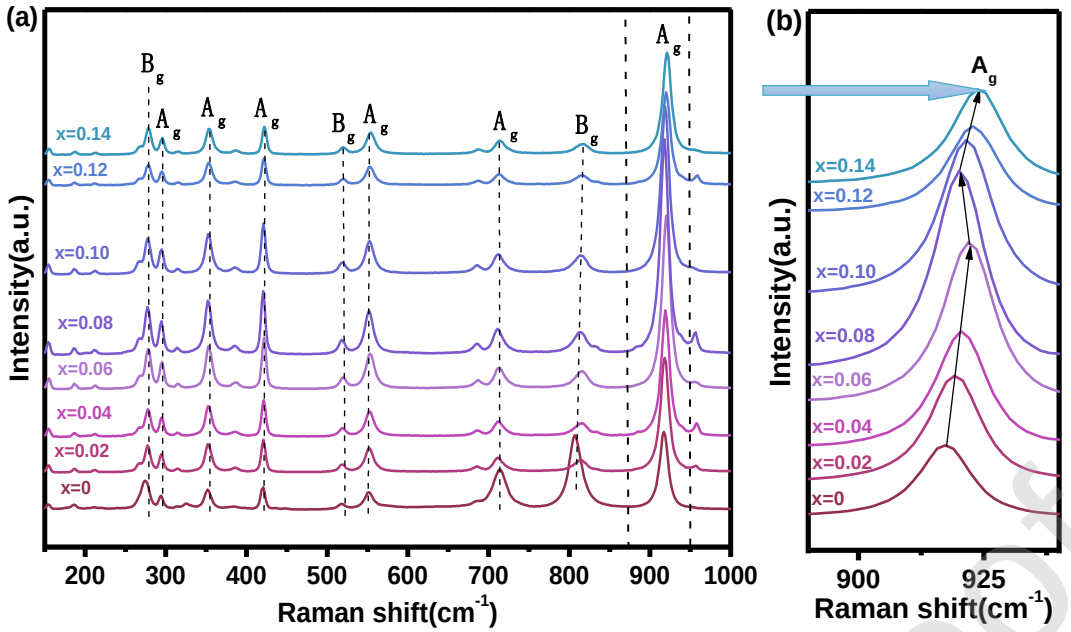

Fig.6 (a) Raman scattering spectroscopy of the $Mg_{1-x}Na_{2x}WO_4$ ceramics in various x and sintered at 875 °C; (b) The amplified profile of the stretch mode Ag.

Raman spectroscopy is an effective method to probe the local crystal structure and phonon vibration characteristics of ceramics [19, 20]. Fig. 6(a) shows the Raman spectra obtained at room temperature for the $Mg_{1-x}Na_{2x}WO_4$ ceramics sintered at 875 °C. The Raman vibrational modes of the samples with Na^+ / Mg^{2+} substitution were nearly the same as those of the pure $MgWO_4$, which indicated that other phases were present in smaller content and had little influence on the vibrational modes of the $Mg_{1-x}Na_{2x}WO_4$ ceramics. According to group-theory analysis, the wolframite structure of $MgWO_4$ has 36 vibrational modes, 18 of which are Raman active (even vibrations *g*) and 18 of which are infrared active (odd vibrations *u*) at the Γ point: Γ= 8Ag + 10Bg + 8Au + 10Bu [19]. The Raman spectrum of $Mg_{1-x}Na_{2x}WO_4$ ceramics contained a strong phonon at around 917cm^{-1}, which corresponded to the symmetric Ag internal vibration of the WO_6 octahedron [21]. Most previous results indicated that the physical properties of the oxygen octahedron as revealed by Raman Ag measurements, strongly influenced the microwave performance [22]. The stretching mode (Ag with a wave-number around 917 cm^{-1}) of the $Mg_{1-x}Na_{2x}WO_4$ ceramics

could be used to deduce the properties of the WO_6 octahedron, allowing the correlation between the microwave dielectric properties to be examined. The amplified profile of the stretch mode Ag (around 917 cm^{-1}) is shown in Fig. 6(b), the change of Raman shift was used to further understand how the relative permittivity of the samples were affected by the concentration of Na.

3.5 Microwave dielectric properties analysis

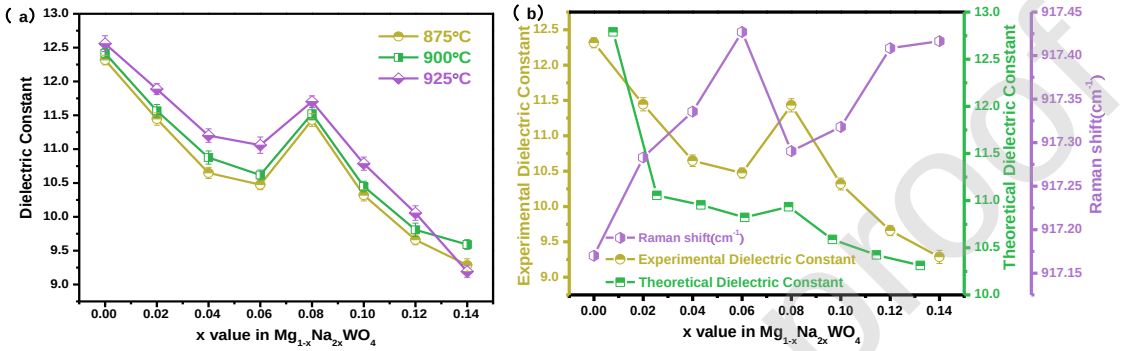

Fig.7 (a) The relative dielectric constants of the $Mg_{1-x}Na_{2x}WO_4$ ($0 \le x \le 0.14$) ceramics sintered at 875 °C, 900 °C and 950 °C; (b) The relationship between experimental relative permittivity values of the $Mg_{1-x}Na_{2x}WO_4$ ceramics sintered at 875°C, and the theoretical permittivity and Raman shift of the stretch mode (Ag with wave-number around 917 cm^{-1}).

It is known that ε_r is related to the molecular polarizability and the second phase [16, 23]. The variation of ε_r with different Na^+ substitution content in $Mg_{1-x}Na_{2x}WO_4$ ($0 \le x \le 0.14$) is revealed in Fig. 7(a). Obviously, with increasing Na^+ substitution content, dielectric constant tended to decrease, which indicated that Na^+ substitution was more conducive to signal transmission [24]. To study the influence of multiple phases on the dielectric constant of the $Mg_{1-x}Na_{2x}WO_4$ ceramics, the theoretical dielectric constants of $Mg_{1-x}Na_{2x}WO_4$ were obtained using the following mixture rule

formula [16, 26]:

$$\ln\varepsilon_{theo} = V_1\ln\varepsilon_{theo1} + V_2\ln\varepsilon_{theo2} + V_3\ln\varepsilon_{theo3} \quad (5)$$

$$\varepsilon_{theo} = \frac{3V_m + 8\pi\alpha_{theo}}{3V_m - 4\pi\alpha_{theo}} \quad (6)$$

$$\alpha_{theo}(A_xB_yC_z) = \alpha_A \times x + \alpha_B \times y + \alpha_C \times z \quad (7)$$

where V_1, V_2, V_3 and ε_{theo1}, ε_{theo2}, ε_{theo3} represent the volume fraction and theoretical dielectric constant of each phase [25-27]; V_m and α_{theo} are the molecular volume and theoretical ionic polarizability of each phase [25]; $\alpha_A, \alpha_B, \alpha_C$ and x, y, z represent the polarizability of each ion in the molecule and the number of each ion in the molecule [28], respectively. As shown in Figure 7(b), the theoretical permittivity trend was consistent with that of the measured permittivity, indicating that the permittivity of $Mg_{1-x}Na_{2x}WO_4$ was mainly affected by the multiple phases. The relationship between the Raman shift and the dielectric constant could be expressed by the following formula [13]:

$$\varepsilon_r(0,\S,K) = \frac{\Omega_p^2\, exp[\lambda(E_F^0 - \S)]}{\omega(\S,k)} \quad (8)$$

where Ω_p is the plasma frequency, ε_r is the dielectric constant and ω is the phonon frequency. According to formula (8), dielectric constant was inversely proportional to the Raman shift, which was consistent with the experimental results shown in Fig. 7(b) and indicated that the relative permittivity was positively correlated with the molecular polarizability [29]. Therefore, the relative permittivity of LTCC could be adjusted by means of various ceramic composites or ion substitution to change the molecular polarizability.

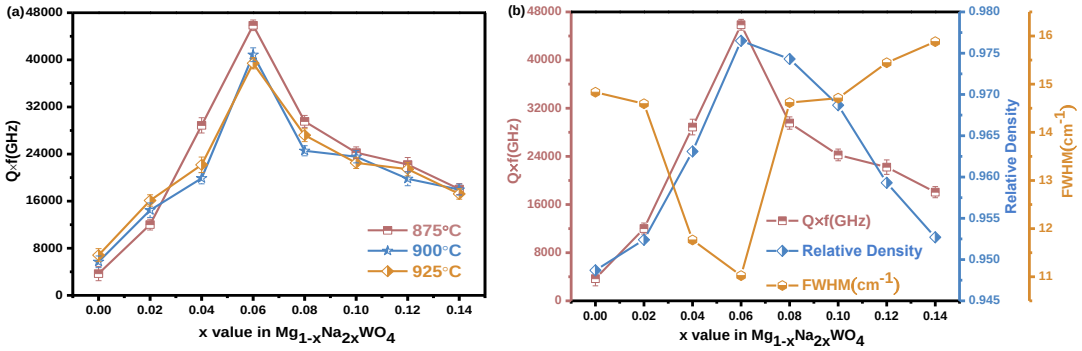

Fig.8 (a) Q×f values of the $Mg_{1-x}Na_{2x}WO_4$ ($0 \le x \le 0.14$) ceramics sintered at 875 °C, 900 °C and 950 °C; (b) The relationship between Q×f values of the $Mg_{1-x}Na_{2x}WO_4$ ceramics sintered at 875 °C and relative density and the FWHM of Roman peaks at 917 cm^{-1}.

Q×f value is not only influenced by the extrinsic factors, such as relative density and porosity [30], but also the intrinsic factors, including lattice vibrational modes and bond energy [31-33]. Fig. 8(a) describes Q×f values of the $Mg_{1-x}Na_{2x}WO_4$ ceramics sintered at different temperatures. As shown in Fig. 8(b), at the same sintering temperature with different Na^+ ion contents, Q×f value firstly increased up to the maximum and then decreased, which was consistent with the relative densities. The increase of relative densities mean that the microstructure become more compact and the porosity is lower, corresponding decrease of external loss leads to the increase of Q×f value [34]. And vice versa. The lattice vibrational modes as intrinsic loss was closely related to the Q×f values. The FWHM of the Raman peak at 917 cm−1, which is assigned to $[WO_6]$ vibration is presented in Fig. 8(b). When the FWHM decreased, the coherence and damping behavior of the Ag stretching vibration weakened, which made $Q \times f$ value increase [35]. Obviously, proper Na^+ substitution could not only reduce the sintering temperature, but also reduce the dielectric loss and improve the

Q×f value of the samples.

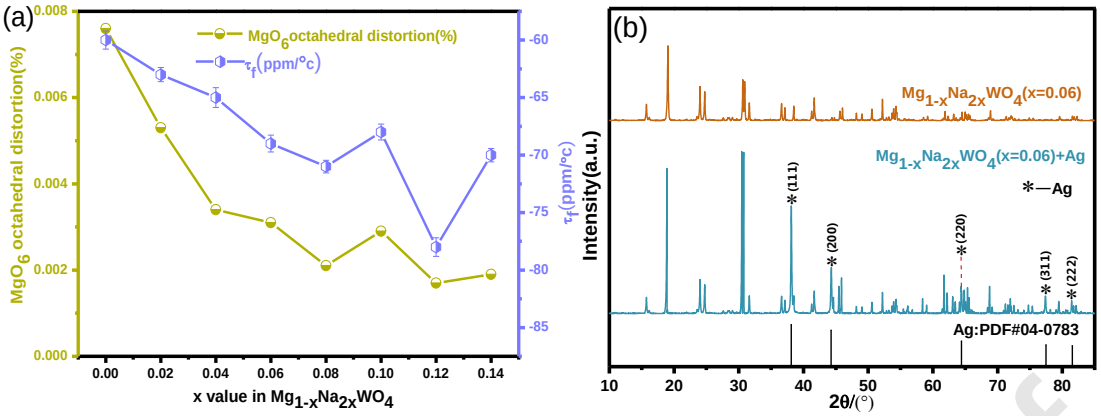

Fig. 9(a) τ_f values and MgO_6 octahedron distortions of the $Mg_{1-x}Na_{2x}WO_4$ ceramics sintered at 875°C; (b) X-ray diffraction of the $Mg_{1-x}Na_{2x}WO_4$ (x=0.06) ceramic co-fired with 20wt% Ag.

τ_f values of the $Mg_{1-x}Na_{2x}WO_4$ ceramics sintered at 875 °C are shown in Fig. 9(a). With the substitution of Na^+ for Mg^{2+} increased, τ_f values became negative because of the presence of [MgO_6] octahedron distortion. It was reported that τ_f mainly depends on the dielectric constant temperature coefficient (τ_ε) [6, 11], and τ_ε was found to be positively correlated with [MgO_6] octahedron distortion (δ) [36, 37], which were calculated as follows [34]:

$$\delta=\frac{1}{6}\sum\left(\frac{R_i-R_A}{R_A}\right)^2 \qquad (9)$$

where R_A and R_i represent the average bond length and bond length in the [MgO_6] octahedron. Therefore, theoretically, the τ_f is directly proportional to the [MgO_6] octahedral distortions, which is also consistent with the experimental results shown in Fig. 9(a). Moreover, the XRD pattern of $Mg_{1-x}Na_{2x}WO_4$ (x=0.06) ceramic sintered with 20wt% Ag at 875 ℃ was shown in Fig. 9(b), indicating that they had a good co-firing compatibility. In the following study, ion substitution could be used to change the [MgO_6] octahedron distortion to obtain the τ_f value near zero, and then

the $Mg_{1-x}Na_{2x}WO_4$ ceramic would be a good candidate for LTCC substrate materials.

4. Conclusions

The microwave dielectric properties of $Mg_{1-x}Na_{2x}WO_4$ (x = 0-0.14) ceramics were explored by using Rietveld refinement and Raman spectroscopy. The substitutions of Na^+ for Mg^{2+} exerted evident effects on the microstructure and microwave dielectric properties. The proper substitution of Na^+ reduced the sintering temperature of $Mg_{1-x}Na_{2x}WO_4$ ceramics, promoted densification of microstructure and relative density of the samples, so as to reduce the dielectric loss of samples and improve Q×f values. It was found that with increasing Na^+ substitution content, the decrease of relative dielectric constant was closely related to the existence of multiphase and molecular polarizability through fitting the Raman spectra. τ_f values became more negative, which was largely due to the distortion of $[MgO_6]$ octahedron. When x=0.06, the $Mg_{1-x}Na_{2x}WO_4$ (x=0.06) ceramic sintered at 875°C achieved the best performance with ε_r= 10.474, $Q\times f$ = 45,868 GHz and τ_f = −69 ppm/ºC, and also showed great chemical compatibility with the commonly used Ag electrode. Accordingly, the $Mg_{1-x}Na_{2x}WO_4$ (x=0.06) ceramic could be a promising candidate for LTCC applications.

Acknowledgements

This work was supported by the National Natural Science Foundation of China under Grant Nos. 61771104, U1809215 and 61871069.

Declaration of interests

The authors declare that they have no known competing financial interests or personal relationships that could have appeared to influence the work reported in this paper.

References

[1] Y. Lai, H. Su, G. Wang, X. Tang, X. Huang, X. Liang, H. Zhang, Y. Li, K. Huang, X.R. Wang, Low- temperature sintering of microwave ceramics with high Qf values through LiF addition, Journal of the American Ceramic Society, 102 (2019) 1893-1903.

[2] B.K. Choi, S.W. Jang, E.S. Kim, Dependence of microwave dielectric properties on crystallization behaviour of $CaMgSi_2O_6$ glass-ceramics, Materials Research Bulletin, 67 (2015) 234-238.

[3] Y.-B. Guo, J.-T. Ma, J.-X. Zhao, K. Du, Z.-T. Fang, Y.-Q. Zheng, W.-Z. Lu, W. Lei, Low-temperature sintering and microwave dielectric properties of CaSn $SiO_{(3+2)}$-based positive τf compensator, Ceramics International, 44 (2018) 18209-18212.

[4] X.-Q. Song, K. Du, X.-Z. Zhang, J. Li, W.-Z. Lu, X.-C. Wang, W. Lei, Crystal structure, phase composition and microwave dielectric properties of $Ca_3MSi_2O_9$ ceramics, Journal of Alloys and Compounds, 750 (2018) 996-1002.

[5] Y.-j. Gu, X.-h. Yang, X. Wang, J.-l. Huang, Q. Li, L.-h. Li, X.-l. Li, B.-h. Kim, Low temperature sintering and dielectric properties of Li_2MgTiO_4 microwave ceramics with $BaCu(B_2O_5)$ addition for LTCC applications, Journal of Materials Science: Materials in Electronics, 30 (2019) 18025-18030.

[6] X.-Q. Song, K. Du, J. Li, X.-K. Lan, W.-Z. Lu, X.-H. Wang, W. Lei, Low-fired fluoride microwave dielectric ceramics with low dielectric loss, Ceramics

International, 45 (2019) 279-286.

[7] M.T. Sebastian, H. Jantunen, Low loss dielectric materials for LTCC applications: a review, International Materials Reviews, 53 (2013) 57-90.

[8] R.C. Pullar, S. Farrah, N.M. Alford, $MgWO_4$, $ZnWO_4$, $NiWO_4$ and $CoWO_4$ microwave dielectric ceramics, Journal of the European Ceramic Society, 27 (2007) 1059-1063.

[9] J.J.B. L.Wang, Effect of $Na_2W_2O_7$ addition on low-temperature sintering and microwave dielectric properties of $CaWO_4$, Materrials Letters, 65 (2011) 726-728.

[10] H.-W. Chen, H. Su, H.-W. Zhang, T.-C. Zhou, B.-W. Zhang, J.-F. Zhang, X.-l. Tang, Low-temperature sintering and microwave dielectric properties of $(Zn_{1-x}Co_x)_2SiO_4$ ceramics, Ceramics International, 40 (2014) 14655-14659.

[11] X.-Q. Song, W.-Z. Lu, X.-C. Wang, X.-H. Wang, G.-F. Fan, R. Muhammad, W. Lei, Sintering behaviour and microwave dielectric properties of $BaAl_{2-2x}(ZnSi)_xSi_2O_8$ ceramics, Journal of the European Ceramic Society, 38 (2018) 1529-1534.

[12] X. Yuan, X. Xue, H. Wang, Preparation of ultra- low temperature sintering ceramics with ultralow dielectric loss in $Na_2O–WO_3$ binary system, Journal of the American Ceramic Society, 102 (2019) 4014-4020.

[13] H. S, Y. Lai, G. Wang, X. Tang, X. Liang, X. Huang, Y. Lia], H. Zhang, Ch. Ye, X. R. Wang, Improved microwave dielectric properties of $CaMgSi_2O_6$ ceramics through CuO doping, Journal of Alloys and Compounds, 772 (2019) 40-48.

[14] T. Qin, C. Zhong, Y. Qin, B. Tang, S. Zhang, Low-temperature sintering

mechanism and microwave dielectric properties of $ZnAl_2O_4$-LMZBS composites, Journal of Alloys and Compounds, 797 (2019) 744-753.

[15] H. Li, X. Chen, P. Zhang, B. Tang, S. Yu, J. Lu, S. Zhang, Influence of Mn^{2+} introduction on microwave dielectric properties of $CaMgSi_2O_6$ ceramic, Ceramics International, 45 (2019) 24425-24430.

[16] E. Li, H. Yang, H. Yang, S. Zhang, Effects of Li_2O-B_2O_3-SiO_2 glass on the low-temperature sintering of $Zn_{0.15}Nb_{0.3}Ti_{0.55}O_2$ ceramics, Ceramics International, 44 (2018) 8072-8080.

[17] X. Jing, X. Tang, W. Tang, Y. Jing, Y. Li, H. Su, Effects of Zn^{2+} substitution on the sintering behaviour and dielectric properties of $Li_2Mg_{1-x}Zn_xSiO_4$ ceramics, Applied Physics A, 125 (2019).

[18] Q. Liao, L. Li, X. Ren, X. Ding, E.S. Kim, New Low-Loss Microwave Dielectric Material $ZnTiNbTaO_8$, Journal of the American Ceramic Society, 94 (2011) 3237-3240.

[19] J. Zhang, R. Zuo, Phase structural transition and microwave dielectric properties in isovalently substituted $La_{1-x}Ln_xTiNbO_6$ (Ln=Ce, Sm) ceramics, Ceramics International, 43 (2017) 7065-7072.

[20] W. Li, L. Fang, Y. Tang, Y. Sun, C. Li, Microwave dielectric properties in the $Li_{4+x}Ti_5O_{12}$ ($0 \le x \le 1.2$) ceramics, Journal of Alloys and Compounds, 701 (2017) 295-300.

[21] J. Ruiz-Fuertes, D. Errandonea, S. López-Moreno, J. González, O. Gomis, R. Vilaplana, F.J. Manjón, A. Muñoz, P. Rodríguez-Hernández, A. Friedrich, I.A.

Tupitsyna, L.L. Nagornaya, High-pressure Raman spectroscopy and lattice-dynamics calculations on scintillating $MgWO_4$: Comparison with isomorphic compounds, Physical Review B, 83 (2011).

[22] Q. Liao, L. Li, Structural dependence of microwave dielectric properties of ixiolite structured $ZnTiNb_2O_8$ materials: crystal structure refinement and Raman spectra study, Dalton Trans, 41 (2012) 6963-6969.

[23] M. Xiao, Y. Wei, Q. Gu, Z. Zhou, P. Zhang, Relationships between bond ionicity, lattice energy, bond energy and the microwave dielectric properties of $La(Nb_{1-x}Ta_x)O_4$ (x = 0–0.10) ceramics, Journal of Alloys and Compounds, 775 (2019) 168-174.

[24] H. Yu, J. Liu, M. Zeng, L. He, Structure and dielectric properties of zinc borate glass–ceramics modified by magnesium, Journal of Materials Science: Materials in Electronics, 27 (2016) 7109-7114.

[25] K. Du, X.-Q. Song, J. Li, J.-M. Wu, W.-Z. Lu, X.-C. Wang, W. Lei, Optimised phase compositions and improved microwave dielectric properties based on calcium tin silicates, Journal of the European Ceramic Society, 39 (2019) 340-345.

[26] H. Ren, S. Jiang, M. Dang, T. Xie, H. Tang, H. Peng, H. Lin, L. Luo, Investigating on sintering mechanism and adjustable dielectric properties of BLMT glass/$Li_2Zn_3Ti_4O_{12}$ composites for LTCC applications, Journal of Alloys and Compounds, 740 (2018) 1188-1196.

[27] W. Liu, R. Zuo, A novel Li_2TiO_3–Li_2CeO_3 ceramic composite with excellent microwave dielectric properties for low-temperature cofired ceramic applications, Journal of the European Ceramic Society, 38 (2018) 119-123.

[28] H. Guo, L. Fang, X. Jiang, J. Li, F. Lu, C. Li, D. Lupascu, A Novel Low-Firing and Low Loss Microwave Dielectric Ceramic $Li_2Mg_2W_2O_9$ with Corundum Structure, Journal of the American Ceramic Society, 98 (2015) 3863-3868.

[29] N. Khobragade, E. Sinha, S.K. Rout, M. Kar, Structural, optical and microwave dielectric properties of $Sr_{1-x}Ca_xWO_4$ ceramics prepared by the solid state reaction route, Ceramics International, 39 (2013) 9627-9635.

[30] C. Zhang, R. Zuo, J. Zhang, Y. Wang, J. Jones, Structure-Dependent Microwave Dielectric Properties and Middle-Temperature Sintering of Forsterite $(Mg_{1-x}Ni_x)_2SiO_4$Ceramics, Journal of the American Ceramic Society, 98 (2015) 702-710.

[31] J. Zhang, J. Zhai, X. Chou, J. Shao, X. Lu, X. Yao, Microwave and infrared dielectric response of tunable $Ba_{1-x}Sr_xTiO_3$ ceramics, Acta Materialia, 57 (2009) 4491-4499.

[32] P. Zhang, Y. Zhao, W. Haitao, Bond ionicity, lattice energy, bond energy and microwave dielectric properties of $ZnZr(Nb_{1-x}A_x)_2O_8$ (A = Ta, Sb) ceramics, Dalton Trans, 44 (2015) 16684-16693.

[33] S. George, M.T. Sebastian, Synthesis and Microwave Dielectric Properties of Novel Temperature Stable High Q, $Li_2ATi_3O_8$ (A=Mg, Zn) Ceramics, Journal of the American Ceramic Society, 93 (2010) 2164-2166.

[34] Y. Lai, X. Tang, X. Huang, H. Zhang, X. Liang, J. Li, H. Su, Phase composition, crystal structure and microwave dielectric properties of $Mg_{2-x}Cu_xSiO_4$ ceramics, Journal of the European Ceramic Society, 38 (2018) 1508-1516.

[35] K. Xiao, Y. Tang, Y. Tian, C. Li, L. Duan, L. Fang, Enhancement of the cation order and the microwave dielectric properties of $Li_2ZnTi_3O_8$ through composition modulation, Journal of the European Ceramic Society, 39 (2019) 3064-3069.

[36] H. Zheng, G.D.C. Csete de Györgyfalva, R. Quimby, H. Bagshaw, R. Ubic, I.M. Reaney, J. Yarwood, Raman spectroscopy of B-site order–disorder in $CaTiO_3$-based microwave ceramics, Journal of the European Ceramic Society, 23 (2003) 2653-2659.

[37] F. Shi, H. Dong, Correlation of crystal structure, dielectric properties and lattice vibration spectra of $(Ba_{(1-x)}Sr_{(x)})(Zn_{(1/3)}Nb_{(2/3)})O_3$ solid solutions, Dalton Trans, 40 (2011) 6659-6667.